

An electrogenic $\text{Na}^+\text{-HCO}_3^-$ cotransporter (NBC) with a novel COOH-terminus, cloned from rat brain

MARK O. BEVENSEE, BERNHARD M. SCHMITT, INYEONG CHOI,
MICHAEL F. ROMERO, AND WALTER F. BORON
*Department of Cellular and Molecular Physiology, Yale University
School of Medicine, New Haven, Connecticut 06520*

Bevenssee, Mark O., Bernhard M. Schmitt, Inyeong Choi, Michael F. Romero, and Walter F. Boron. An electrogenic $\text{Na}^+\text{-HCO}_3^-$ cotransporter (NBC) with a novel COOH-terminus, cloned from rat brain. *Am J Physiol Cell Physiol* 278: C1200–C1211, 2000.—We screened rat brain cDNA libraries and used 5' rapid amplification of cDNA ends to clone two electrogenic $\text{Na}^+\text{-HCO}_3^-$ cotransporter (NBC) isoforms from rat brain (rb1NBC and rb2NBC). At the amino acid level, one clone (rb1NBC) is 96% identical to human pancreas NBC. The other clone (rb2NBC) is identical to rb1NBC except for 61 unique COOH-terminal amino acids, the result of a 97-bp deletion near the 3' end of the open-reading frame. Using RT-PCR, we confirmed that mRNA from rat brain contains this 97-bp deletion. Furthermore, we generated rabbit polyclonal antibodies that distinguish between the unique COOH-termini of rb1NBC (αrb1NBC) and rb2NBC (αrb2NBC). αrb1NBC labels an ~130-kDa protein predominantly from kidney, and αrb2NBC labels an ~130-kDa protein predominantly from brain. αrb2NBC labels a protein that is more highly expressed in cortical neurons than astrocytes cultured from rat brain; αrb1NBC exhibits the opposite pattern. In expression studies, applying 1.5% $\text{CO}_2/10$ mM HCO_3^- to *Xenopus* oocytes injected with rb2NBC cRNA causes 1) pH_i to recover from the initial CO_2 -induced acidification and 2) the cell to hyperpolarize. Subsequently, removing external Na^+ reverses the pH_i increase and elicits a rapid depolarization. In the presence of 450 μM DIDS, removing external Na^+ has no effect on pH_i and elicits a small hyperpolarization. The rate of the pH_i decrease elicited by removing Na^+ is insensitive to removing external Cl^- . Thus rb2NBC is a DIDS-sensitive, electrogenic NBC that is predominantly expressed in brain of at least rat.

intracellular pH; pH regulation; alternative splice variant; bicarbonate; sodium

THE REGULATION OF pH is important in the central nervous system (CNS) because changes in either the pH of the intracellular fluid (pH_i) or the pH of the extracellular fluid (pH_{ECF}) can alter the level of neuronal activity (see Refs. 15 and 31). In general, decreases in pH_{ECF} inhibit, whereas increases in pH_{ECF} stimulate neuronal firing, probably because many cellular functions are sensitive to changes in pH_{ECF} and/or accompanying changes in pH_i . For example, decreases in pH_{ECF}

inhibit many voltage- and ligand-activated ion channels (see Refs. 43 and 49). The relationship between changes in brain pH and neuronal activity is complicated, however, because neuronal firing itself elicits changes in both pH_i and pH_{ECF} . Neuronal firing typically causes a decrease in the pH_i of the neurons involved and a corresponding increase in pH_{ECF} due to acid-base transport across neuronal plasma membranes. The activity-evoked pH_i decrease of neurons can occur via HCO_3^- efflux through GABA_A -stimulated Cl^- channels that are permeable to HCO_3^- (13, 14, 25, 26) and also via H^+ influx mediated by the $\text{Ca}^{2+}\text{-H}^+$ pump (27, 28, 39, 42, 48). Because neurons and astrocytes are in such close apposition to one another in the CNS, the increase in pH_{ECF} will also increase the pH_i of the inactive adjacent cells by altering the activity of acid-base transporters that are sensitive to extracellular pH. For instance, increases in pH_{ECF} typically stimulate acid extruders (e.g., Na^+/H^+ exchanger and $\text{Na}^+\text{-HCO}_3^-$ cotransporter with a 1:2 or 1:1 $\text{Na}^+:\text{HCO}_3^-$ stoichiometry) that move H^+ out of or base equivalents such as HCO_3^- or OH^- into cells. In addition, increases in pH_{ECF} can inhibit acid loaders (e.g., $\text{Cl}^-/\text{HCO}_3^-$ exchanger) that move H^+ into or base equivalents out of cells. Therefore, acid-base transport mechanisms in brain cells not only contribute to the long-term $\text{pH}_i/\text{pH}_{\text{ECF}}$ homeostasis of the CNS, but they also contribute to transient changes in $\text{pH}_i/\text{pH}_{\text{ECF}}$ during neuronal firing.

Some of the most powerful pH_i -regulating transporters in neurons and glia are HCO_3^- dependent (see Refs. 5, 18, 19, and 35). For example, in freshly dissociated CA1 neurons with a relatively low resting pH_i from immature rats, a Na^+ -driven $\text{Cl}^-/\text{HCO}_3^-$ exchanger is the predominant acid extruder responsible for the pH_i recovery from an acid load in the presence of $\text{CO}_2/\text{HCO}_3^-$ (38). Similarly, in cultured hippocampal neurons, the activity of a HCO_3^- -dependent acid extruder appears to be about twofold greater than that of the Na^+/H^+ exchanger during the pH_i recovery from an acid load in the presence of $\text{CO}_2/\text{HCO}_3^-$ (30). HCO_3^- -dependent transporters also play an important role in regulating the pH_i of glial cells. For instance, an electrogenic $\text{Na}^+\text{-HCO}_3^-$ cotransporter with a 1:2 stoichiometry was first documented in leech glial cells (20, 21). Subsequently, similar $\text{Na}^+\text{-HCO}_3^-$ cotransporters have been identified in several other nonmammalian glial cells, and evi-

The costs of publication of this article were defrayed in part by the payment of page charges. The article must therefore be hereby marked "advertisement" in accordance with 18 U.S.C. Section 1734 solely to indicate this fact.

dence has been presented for the existence of $\text{Na}^+\text{-HCO}_3^-$ cotransporters in mammalian glial cells (see Refs. 18, 19, and 35). More recently, we have shown that the Na^+ -driven HCO_3^- transporter in cultured hippocampal astrocytes elicits membrane voltage changes of a magnitude that is consistent with the transporter being an electrogenic $\text{Na}^+\text{-HCO}_3^-$ cotransporter with a 1:2 stoichiometry (4, 7). As proposed by Chesler (15) and Ransom (31), an electrogenic $\text{Na}^+\text{-HCO}_3^-$ cotransporter in glial cells may be stimulated by cell depolarization elicited by increases in the extracellular K^+ concentration ($[\text{K}^+]_o$) in response to neuronal activity. Such a depolarization-induced alkalization indeed occurs in cultured astrocytes exposed to high- $[\text{K}^+]_o$ solutions (10). The accompanying decrease in pH_{ECF} could slow further neuronal firing. Clearly, HCO_3^- transport mechanisms are abundant in the nervous system, and they are likely to regulate the pH of the neurons, the glial cells, and the surrounding extracellular fluid, particularly during neuronal activity.

Except for the anion exchangers (AEs), little was known about HCO_3^- transporters at the molecular level until Romero et al. (34) expression cloned the electrogenic $\text{Na}^+\text{-HCO}_3^-$ cotransporter (NBC) from *Ambystoma* kidney (akNBC). Subsequently, others have identified NBCs from human kidney (11), rat kidney (12, 33), human pancreas (1) and heart (17), human skeletal muscle (29), and rat aorta and pulmonary artery (16). Rat kidney NBC (rkNBC) is 33% identical to rat AE1, and both proteins are predicted to possess at least 10 membrane-spanning segments. Several investigators have detected NBC-related mRNA in brain from rat and human, based on Northern blotting (2, 11, 12, 17, 33, 36) and in situ hybridization (24, 36). Investigators have also identified NBC-related proteins in rat brain, based on immunoblotting (22, 36) and immunolocalization (36).

In the present study, we cloned two NBC-related cDNAs from rat brain (rb1NBC and rb2NBC), based on their homology to rkNBC. At the protein level, rb1NBC is 96% identical to the NBC encoded by the cDNA previously cloned from human pancreas and heart (hpNBC). rb2NBC is identical to rb1NBC at the cDNA level, except for a 97-bp deletion near the 3' end of its open-reading frame (ORF). The resultant frame shift yields a protein with 61 unique COOH-terminal amino acids (AA); these replace the 46 COOH-terminal AA of rb1NBC. At the protein level, rb2NBC is 92% identical to hpNBC. We have generated rabbit polyclonal antibodies that distinguish between the COOH-termini of rb1NBC and rb2NBC. In rat, a protein with the COOH-terminus of rb2NBC is predominantly expressed in brain and the protein is expressed heavily in cultured cortical neurons compared with astrocytes. When expressed in *Xenopus* oocytes, rb2NBC displays all of the hallmarks of a DIDS-sensitive, electrogenic $\text{Na}^+\text{-HCO}_3^-$ cotransporter.

Portions of this work have been published in abstract form (6).

METHODS

Cloning

Library screening. We screened the following two size-selected, λ ZAP II cDNA libraries: 1) an oligo(dT)-primed rat brain cDNA library (λ RB-L; kindly provided by Dr. Terry Snutch, Univ. of British Columbia) and 2) a random-primed rat forebrain cDNA library (λ ZAPRFB; kindly provided by the Molecular Neurobiology Laboratory, Salk Institute, La Jolla, CA). Both libraries were first titered and then plated at $\sim 50,000$ plaque-forming units per plate. DNA from the plaques was transferred and ultravioletly cross-linked to Hybond-N nylon membranes (Amersham Pharmacia Biotech, Piscataway, NJ). Subsequently, the membranes were probed at 68°C for 15–18 h with a [^{32}P]cDNA probe (see below) in Express-Hyb (Clontech Laboratories, Palo Alto, CA). Membranes were then washed with 1) $2\times$ saline sodium citrate (SSC)/0.05% SDS [1-, 5-, and 15-min washes at room temperature (RT), then 2×20 -min washes at 44°C] and 2) $0.1\times$ SSC/0.1% SDS (3×20 -min washes at 44°C). Washed filters were wrapped in Saran wrap and exposed to Kodak X-Omat film (Kodak, Rochester, NY) overnight. Positive plaques were isolated and replated, and a secondary screening was performed as described above. Positive single plaques from the secondary screen were isolated, and the corresponding pBluescript SK(-) phagemids were excised ("rescued") from the λ ZAP II vector using the F1 helper phage (Stratagene, La Jolla, CA). The cloned cDNA inserts within the phagemids were sequenced by the Keck Sequencing Center (New Haven, CT) using fluorescent dideoxy sequencing. All nucleic acid sequences were analyzed with DNAsis (Hitachi Software, San Bruno, CA).

Probes for cDNA library screening. For the λ RB-L cDNA library screen, the cDNA probe was obtained by PCR, using as a template cDNA from rat hippocampal astrocytes; the primers were degenerate primers to a portion of the rkNBC ORF. Hippocampal astrocytes were grown as previously described (7), and total RNA was harvested using the TRIzol Reagent (GIBCO-BRL Life Technologies, Gaithersburg, MD). mRNA was then isolated using the Oligotex mRNA kit (Qiagen, Valencia, CA). The sense degenerate primer [5'-gCTAT(A/T/C)CCggCTTTgCT(T/C)GTIACC-3'] was to nucleotides 2221–2244 of the rkNBC ORF; the antisense degenerate primer [5'-gAg(g/A)TCgTgCTgggA(g/A)AAIAG-3'] was to nucleotides 2825–2845 of the rkNBC ORF. The PCR product was then labeled with [^{32}P]CTP by random-hexamer priming (GIBCO-BRL Life Technologies).

For the λ ZAPRFB cDNA library screen, the probe was a ^{32}P -labeled, 577-bp portion of rkNBC (bp 1027–1603 of the ORF). *EcoR* I and *Sca* I restriction enzymes were used to excise this probe from a pBluescript vector containing a partial-length clone obtained from the λ RB-L cDNA library screen described above. The probe was ^{32}P -labeled as described above.

5' Rapid amplification of cDNA ends. The above library screening yielded two types of clones with different 3' ends, but lacking the 5' ends of the ORF. The 5' ends of the two types of clones were obtained by using two rounds of 5' rapid amplification of cDNA ends (5'-RACE; GIBCO-BRL Life Technologies) using mRNA from an adult rat brain. The brain was excised from a decapitated rat and was immediately homogenized in TRIzol Reagent. Total RNA and mRNA were then isolated as described above for rat hippocampal astrocytes.

In the first round of 5'-RACE, cDNA from rat brain mRNA was generated using RT and the gene-specific primer 5'-gTCAGACATCAAggTggCgATggCTCTTCC-3'. After tailing the

cDNA with a poly(C) homopolymer, we used PCR to amplify the cDNA using a primer complementary to the poly(C) tail and a primer to an internal gene-specific sequence (5'-gggCACAggCACCTCAGTCAGggC-3'). The former primer is engineered to contain an additional "abridged" sequence. The cDNA was further amplified using PCR and primers to the abridged sequence and a second internal gene-specific sequence (5'-AgTgTCCAAGAAgTCAACCTCCCC-3'). The same methodology was used to perform the second round of 5'-RACE, using 5'-TgTCTTCCCAATgTCAGCCAgggA-3' to make the cDNA and primers to internal gene-specific sequences (5'-ggATTTCTTggTTTgATgTCggTg-3' and 5'-CCg-CAGcAgCgTATAggTgAC-3') to amplify the cDNA. Full-length clones were amplified using RT-PCR and primers to the beginning and to the end of the ORFs of the two clones. The PCR products were subcloned into pCR2.1 (Invitrogen, Carlsbad, CA) and sequenced.

Generating Polyclonal Antibodies

Immunogens were prepared using the maltose-binding protein (MBP) fusion-protein system, as described by Schmitt et al. (37). Briefly, a purified PCR product encoding either the COOH-terminal 46 AA of rb1NBC or the COOH-terminal 61 AA of rb2NBC was subcloned into the expression vector pMAL-c2 (NEB, Beverly, MA). DH5 α *Escherichia coli* (GIBCO-BRL Life Technologies) were transfected with the pMAL-c2 constructs, grown at 37°C in Luria-Bertani media containing 100 $\mu\text{g}/\text{ml}$ ampicillin, and supplemented with 300 μM isopropylthiogalactoside to induce expression of the fusion-protein gene. The *E. coli* were then harvested and sonicated in a homogenization buffer (HB: 300 mM sucrose, 10 mM Tris·HCl, and 1 mM EGTA, pH 7.4) containing the following protease inhibitors: 1 mM phenylmethylsulfonyl fluoride, 1 μM pepstatin A, and 1 μM leupeptin. The sonicated suspension was cleared from debris by centrifugation, diluted 1:5 with HB, and run through a column of amylose beads (NEB). The resin was then washed with HB to eliminate unbound proteins. The fusion protein was eluted from the resin with HB supplemented with 10 mM maltose, and then was quantitated with the bicinchoninic acid (BCA) kit (Pierce, Rockford, IL). Purified fusion protein (200 μg) in complete Freund's adjuvant was injected in rabbits by Yale Veterinary Services. Booster injections of 25 to 100 μg fusion protein in incomplete Freund's adjuvant were given each month.

Immunoblotting

Our immunoblotting procedure is described in greater detail by Schmitt et al. (37).

Culturing astrocytes and neurons. We cultured astrocytes from rat cortex as previously described for astrocytes from rat hippocampus (7). We obtained cultured neurons from rat cortex from Ying Xia and Gabriel G. Haddad (Dept. of Pediatrics, Yale University), who cultured the neurons as described by Xia et al. (50).

Preparing microsomes. Tissues isolated from Sprague-Dawley rats, or cultured astrocytes or neurons scraped from tissue-culture flasks, were placed in ice-cold HB and were homogenized using a Polytron (model PT-MR 3100; Kinematica, Littau, Switzerland). The homogenate was then centrifuged for 15 min at $\sim 600 g$ (4°C) to remove cell debris and nuclei. The supernatant was centrifuged again for 45 min at $\sim 28,000 g$ (4°C) to pellet microsomes containing plasma and organellar membranes. The pellet was resuspended in HB, and the protein concentration was determined with the BCA kit.

Preparing protein from *Xenopus* oocytes. Oocytes injected with either H_2O or cRNA were pooled in an Eppendorf tube

and were suspended in 20 $\mu\text{l}/\text{oocyte}$ of fresh Triton HB (100 mM NaCl, 20 mM Tris·HCl, and 1% Triton X-100, pH 7.6). The oocytes were homogenized with a pellet pestle and were centrifuged for 10 min at $\sim 12,000 g$ (4°C) to pellet cell debris. The protein-containing supernatant was then removed and stored at -70°C .

Gel electrophoresis and protein transfer. Microsomal proteins were separated by SDS-PAGE. Proteins in the gel were transferred to polyvinylidene difluoride membranes (Immobilin-P; Millipore, Bedford, MA) using a semi-dry blotting apparatus (Bio-Rad Laboratories, Richmond, CA) and a discontinuous buffer system. Proteins on membranes were visualized by Coomassie blue staining.

Antibody detection. Membranes were incubated for 30 min at RT in a "blocking" solution (Blotto) that contained PBS (137 mM NaCl, 10 mM Na_2HPO_4 , 1.8 mM KH_2PO_4 , and 2.7 mM KCl, pH 7.4), 5% Carnation dry milk powder (Nestle Food, Glendale, CA), and 0.05% Tween 20. Membranes were then incubated first for 1 h at RT in Blotto containing the primary antibody, and then for 1 h at RT in Blotto containing a 1:3,000 dilution of the secondary antibody [goat α -rabbit-whole IgG-horseradish peroxidase (HRP) (Sigma)]. Membranes were then washed with copious amounts of antibody-free Blotto. In a preabsorption experiment, Blotto containing the primary antibody was mixed for ~ 30 min with 10 $\mu\text{g}/\text{ml}$ fusion protein before being applied to the membranes. Bound HRP was detected by the SuperSignal chemiluminescence detection kit (Pierce), and membranes were exposed to Kodak X-Omat film (Kodak).

Functional Characterization of rb2NBC

Harvesting and injecting oocytes. Stage V/VI oocytes were harvested from female *Xenopus laevis* frogs as described by Romero et al. (33). cDNA encoding rb2NBC was subcloned into the *Xenopus* expression vector pTLN2 (33), and cRNA encoding rb2NBC was transcribed in vitro using the T7 promoter and the mMessage mMachine kit (Ambion, Austin, TX). The cRNA was then capped and purified by phenol/chloroform extraction. The oocytes in OR3 medium (50% Leibovitz L-15 media containing 1 mM L-glutamine and 5 mM HEPES, pH 7.5, supplemented with 5 U/ml penicillin-streptomycin) were visualized with a dissecting microscope and were injected with 50 nl of RNase-free H_2O or solution containing cRNA. The sterile pipettes had tip diameters of 20–50 μm and were backfilled with paraffin oil before being connected to a Drummond "Nanoject" microinjector (Drummond Scientific, Broomall, PA). Injected oocytes were maintained at 18°C and were studied 3–8 days postinjection.

pH_i and membrane potential experiments. Our technique for measuring pH_i and membrane potential (V_m) of oocytes has been described previously (17, 33). pH- and voltage-sensitive microelectrodes were pulled from borosilicate fiber-capillary glass (Warner Instruments, West Haven, CT) using a microelectrode puller (model P-97; Sutter Instrument, Novato, CA). The pH microelectrodes were then dried for at least 2 h at 200°C before being silanized with bis(dimethyl-amino)dimethyl silane vapor. The electrode tips were filled with hydrogen ionophore I-cocktail B (Fluka Chemical), back-filled with a phosphate buffer (150 mM NaCl, 40 mM KH_2PO_4 , and 23 mM NaOH, pH 7.0), and connected to a high-impedance electrometer. The V_m microelectrodes were filled with 3 M KCl and were connected to a high-impedance electrometer. V_m microelectrodes had resistances of 0.2–2 M Ω . All experiments were performed at RT.

An oocyte was stabilized on a nylon-mesh platform placed on the bottom of a flow-through chamber before being impaled with pH- and voltage-sensitive microelectrodes. Solu-

tions to the chamber were changed by a daisy-chained system of computer-actuated five-way valves.

Solutions

The standard ND-96 solution contained (in mM) 96 NaCl, 2 KCl, 1.8 CaCl₂, 1 MgCl₂, and 5 HEPES, and was titrated to pH 7.5 with NaOH. CO₂ (1.5%)/HCO₃⁻ (10 mM)-buffered solutions (pH 7.5) were made by replacing 10 mM NaCl with 10 mM NaHCO₃. In Na⁺-free solutions, the Na⁺ substitute was either *N*-methyl-D-glucammonium (NMDG⁺), choline, or Li⁺. In Cl⁻-free solutions, the Cl⁻ substitute was gluconate, and total Ca²⁺ concentration was increased 3-fold, and total Mg²⁺ concentration was increased 1.5-fold to compensate for chelation by the anion substitute. All chemicals were obtained from Sigma Chemical (St. Louis, MO).

Statistics

Data are reported as means ± SE. Levels of significance were assessed using the paired and unpaired Student's *t*-test. A *P* value < 0.05 was considered significant. Rates of change of pH_i (dpH_i/dt values) were fitted by a line using a least-squares method.

RESULTS

Cloning of Two NBC-Related cDNAs From Rat Brain

Cloning strategy. We screened a rat brain cDNA library (λRB-L) with a [³²P]cDNA fragment of rkNBC and obtained several partial-length clones that fell into two groups. The clones in one group had ORFs that were identical to the corresponding ORF of rkNBC. The clones in the other group had ORFs that were nearly

identical to the corresponding ORF of rkNBC, except for a 97-bp deletion near the 3' end. None of the clones in either group contained the 5' end of the ORF.

We next attempted to obtain the 5'-ORF of each clone by screening a random-primed rat forebrain cDNA library (λZAPRFB) with a [³²P]cDNA fragment of one of the partial-length clones isolated in the first library screen. Although the isolated clones also fell into the same two groups (i.e., those with and without the 97-bp deletion), none of them possessed the missing 5'-ORF. We therefore used two rounds of 5'-RACE to obtain the 5'-ORF of both clones. As shown below, the 5'-ORFs of the two clones are identical to one another and are nearly identical to that of the NBC cloned from human pancreas and heart (hpNBC). We subsequently used PCR and primers to the ends of the two clones to amplify the entire ORFs from rat brain cDNA.

Sequence analysis of rb1NBC and rb2NBC. At the AA level, the clone without the 97-bp deletion (rb1NBC) is 96% identical to hpNBC. This clone has an ORF of 3237 bp, which encodes a protein of 1079 AA. As is the case for the comparable human NBCs, rb1NBC and rkNBC are identical, except that the NH₂-terminal 85 AA in rb1NBC replace the NH₂-terminal 41 AA in rkNBC. As shown in Fig. 1A, the NH₂-terminal 85 AA of rb1NBC and hpNBC are identical except for two AA.

The second clone (rb2NBC) is identical to rb1NBC, except for a 97-bp deletion near the 3'-ORF. This deletion causes a frame shift that extends the ORF (Fig. 1B) so that the ORF of rb2NBC contains 3,282 bp

A

rb1NBC:	MEDEAVLDRGASFLKHVCEDEEEVEGHHTIYIGVHVPKSYRRRRRHKRKAGHKEKKEKERISENYSKSDSVE	71
hpNBC:	MEDEAVLDRGASFLKHVCEDEEEVEGHHTIYIGVHVPKSYRRRRRHKRKAGHKEKKEKERISENYSKSDSIE	71
rb1NBC:	NADESSSSILKPLI...	85
hpNBC:	NADESSSSILKPLI...	85

B

rb1NBC:	...AAAGGAAGTCTGGATAGCGACAACGACGATCTGACTGCCCATACTCAGAAAAGTCCCAGTATTAAAAAT	3140
rb2NBC:	...AAAGGAAGTCTGGATAGCGACAACGACGAT-----	3099
rb1NBC:	TCCAATGGACATCACGGAACAGCAACCTTTCCTAAGTGATAACAAACCTTGGACAGAGAAAGATCCTCAA	3211
rb2NBC:	-----GAGAAAGATCCTCAA	3114
rb1NBC:	CATTCCCTTGAACGCCACACATCATGCTGATAAAAATTCCTTTCCTTGAGTCACTGGGTTTACCAGTCCCTCC	3282
rb2NBC:	CATTCCCTTGAACGCCACACATCATGCTGATAAAAATTCCTTTCCTTGAGTCACTGGGTTTACCAGTCCCTCC	3185
rb1NBC:	AAGATCTCCAGTGAAAGTCGTGCCTCAAATAGAAATAGAATTGAGTCTGAAGACAACGATTATCTTTGGA	3353
rb2NBC:	AAGATCTCCAGTGAAAGTCGTGCCTCAAATAGAAATAGAATTGAGTCTGAAGACAACGATTATCTTTGGA	3256
rb1NBC:	GGAACAAGGGAACAGAAACCACGTTGTAA	3382
rb2NBC:	GGAACAAGGGAACAGAAACCACGTTGTAA	3285

C

rb1NBC:	...KGSLSDDNDSDCYPYSEKVFPSIKIPMDITEQQPFLSDNKPLDRRSSTFLERHTSC	1079
rb2NBC:	...KGSLSDDNDDEKDPQHSLNATHADKIPFLESGLPSPRSPVVKVVPQIRIELESEDNDYLWRNKGTETTL	1094

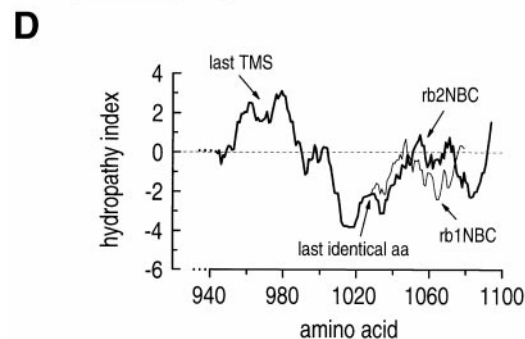


Fig. 1. Rat brain 1 Na⁺-HCO₃⁻ cotransporter (rb1NBC) and rb2NBC are nearly identical to human pancreas (hp) NBC at the NH₂-terminus but are different from one another at the COOH-terminus. **A**: comparison of the NH₂-termini of rb1NBC and hpNBC. Gray regions in **A** and **C** highlight identical amino acids (AA). **B**: comparison of the 3' open-reading frames of rb1NBC (without the deletion) and rb2NBC (with the 97-bp deletion). **C**: comparison of the COOH-termini of rb1NBC and rb2NBC. Because of the 97-bp deletion in rb2NBC (**B**), the 61 COOH-terminal AA replace the 46 COOH-terminal AA in rb1NBC. **D**: comparison of the Kyte-Doolittle hydropathy plots of the COOH-terminal 136 AA of rb1NBC (thin trace) and the COOH-terminal 151 AA of rb2NBC (thick trace). TMS, transmembrane segment.

that encode a protein of 1,094 AA. Thus the first 1,033 AA of rb1NBC and rb2NBC are identical. However, because of the frame shift, the COOH-terminal 61 AA of rb2NBC differ from the last 46 AA of rb1NBC (Fig. 1C); overall, rb2NBC is 95% identical to rb1NBC. rb2NBC is 92% identical to hpNBC. The unique COOH-terminal 61 AA of rb2NBC contain consensus sequence sites for NH_2 -linked glycosylation (AA 1042–1044) and myristylation (AA 1089–1094). Inasmuch as the current models for the AE and NBC families predict that the COOH-terminus is cytoplasmic, AA 1042–1044 are presumably not available for NH_2 -linked glycosylation. As shown in Fig. 1D, the hydropathy plots of the COOH-terminal 136 AA of rb1NBC (without the frame shift) and the COOH-terminal 151 AA of rb2NBC (with the frame shift) are fairly similar.

rb2NBC mRNA Expressed in Rat Brain

We used RT-PCR techniques to confirm that rb2NBC (i.e., with the 97-bp deletion) is present in mRNA isolated from rat whole brain. After synthesizing rat brain cDNA by reverse transcribing mRNA, we amplified the cDNA using PCR techniques and primers to sequences flanking the 97-bp deletion. Analyzing a portion of the reaction on a 1.5% agarose gel, we observed two bands (Fig. 2). The ~640-bp band was the expected product from rb1NBC (without the deletion), and the ~540-bp band was the expected product from rb2NBC (with the 97-bp deletion). We subcloned and sequenced similar PCR products to confirm their identity. We observed no bands with H_2O as the template in the PCR.

In another series of RT-PCR experiments with cDNA made from isolated regions of rat brain, we used similar primers to detect bands representative of rb1NBC and rb2NBC. In whole brain, cerebral cortex, brainstem diencephalon, and cerebellum, we detected each of the two PCR products (B. M. Schmitt, U. V. Berger, R.

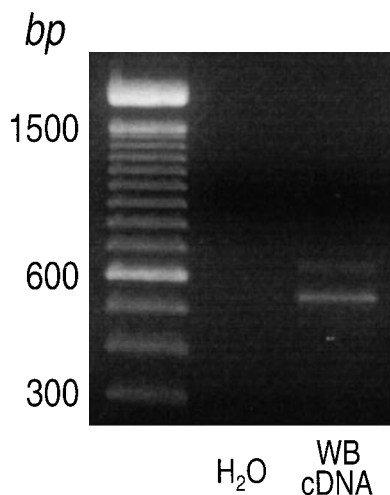


Fig. 2. mRNA containing the 97-bp deletion is present in whole rat brain. RT-PCR was performed using either H_2O (negative control) or whole brain (WB) cDNA as the template, and oligonucleotides flanking the 97-bp deletion as the primers. The products were analyzed on a 1.5% agarose gel.

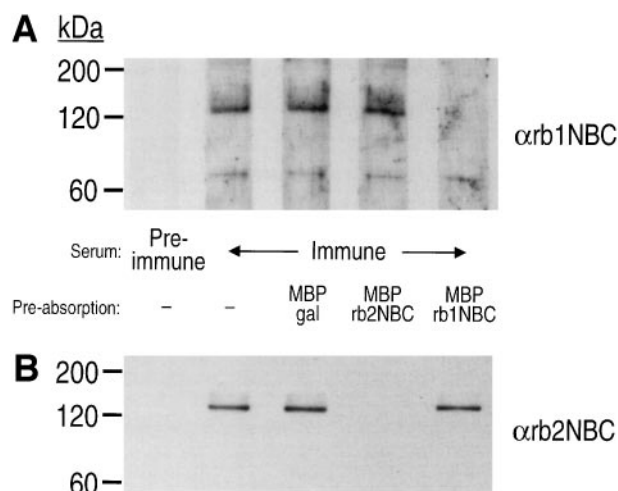


Fig. 3. Antibodies to rb1NBC (αrb1NBC) and rb2NBC (αrb2NBC) label different ~130-kDa proteins from rat brain. *A*: preimmune serum (lane 1) and αrb1NBC exposed to maltose-binding protein (MBP)-rb1NBC (lane 5) failed to label protein, whereas αrb1NBC (lane 2) and αrb1NBC exposed to MBP-gal (lane 3) or MBP-rb2NBC (lane 4) labeled an ~130-kDa protein. Each lane contained ~20 μg total protein. Sera were diluted 1:2,000, and fusion proteins in the preabsorption lanes were used at 10 $\mu\text{g}/\text{ml}$. *B*: preimmune serum (lane 1) and αrb2NBC exposed to MBP-rb2NBC (lane 4) failed to label protein, whereas αrb2NBC (lane 2) and αrb2NBC exposed to MBP-gal (lane 3) or MBP-rb1NBC (lane 5) labeled an ~130-kDa protein. Each lane contained ~20 μg total protein. Sera were diluted 1:15,000, and fusion-proteins in the preabsorption lanes were used at 10 $\mu\text{g}/\text{ml}$.

Douglas, M. O. Bevensee, M. A. Hediger, G. G. Haddad, and W. F. Boron, unpublished observations).

rb2NBC Protein Expressed in Rat Brain

Polyclonal antibodies to rb1NBC and rb2NBC. To determine if rb1NBC and rb2NBC proteins are expressed in rat brain, we generated rabbit polyclonal antibodies that would discriminate between the COOH-termini of the two proteins. We generated two polyclonal antibodies, one against the COOH-terminal 46 AA of rb1NBC (αrb1NBC) and the other against the COOH-terminal 61 AA of rb2NBC (αrb2NBC). We separated microsomal proteins from rat brain by SDS-7.5% PAGE and then immunoblotted the protein with preimmune rabbit serum as well as αrb1NBC (Fig. 3A) and preimmune serum as well as αrb2NBC (Fig. 3B). Neither of the preimmune sera labeled brain protein (Fig. 3, A and B, lane 1). In contrast, both αrb1NBC and αrb2NBC labeled ~130-kDa proteins in brain (Fig. 3, A and B, lane 2). Therefore, rat brain expresses protein containing the COOH-termini of both rb1NBC and rb2NBC.

Recognition of distinct epitopes by αrb1NBC and αrb2NBC . As also shown in Fig. 3, we examined the specificity of labeling by attempting to preabsorb the antibodies with various fusion proteins (Fig. 3, A and B, lanes 3–5). In Fig. 3A, αrb1NBC labeled an ~130-kDa protein even after the antiserum was exposed to the MBP-gal and MBP-rb2NBC fusion proteins (lanes 3 and 4, respectively). In contrast, αrb1NBC failed to label a protein after the serum was exposed to the immunogen, the MBP-rb1NBC fusion protein (Fig. 3A,

lane 5). Note that the labeling of the ~70-kDa protein by αrb1NBC (Fig. 3A, lanes 2–5) is nonspecific because it occurs even in the presence of MBP-rb1NBC (Fig. 3A, lane 5).¹ Thus αrb1NBC labels an ~130-kDa brain protein by recognizing the unique 46 AA of rb1NBC.

We performed a similar competition experiment with αrb2NBC (Fig. 3B). αrb2NBC labeled an ~130-kDa protein even after being exposed to the MBP-gal and MBP-rb1NBC fusion proteins (lanes 3 and 5, respectively). In contrast, αrb2NBC failed to label a protein after we exposed the serum to the immunogen, the MBP-rb2NBC fusion protein (lane 4). Thus αrb2NBC labels a brain protein by recognizing the unique 61 AA of rb2NBC.

Localization of rb1NBC and rb2NBC in rat tissues. To assess the tissue distribution of rb1NBC, we separated microsomal proteins from various tissues of an ~60-day-old male rat by SDS-7.5% PAGE and then immunoblotted the protein with rabbit αrb1NBC (1:1,000 dilution). As observed after an ~2-s film exposure during chemiluminescence detection, αrb1NBC labeled an ~130-kDa protein and weakly labeled ~95- and ~75-kDa proteins in kidney (Fig. 4A). Schmitt et al. (37) observed similar bands in rat kidney using an antibody raised against a larger COOH-terminal epitope of the rkNBC protein. The serum also labeled ~130-, ~110-, and ~95-kDa proteins in small intestine. After a ~3-min film exposure (data not shown), the serum also labeled an ~130-kDa protein in brain, ~140-, ~110-, and ~95-kDa proteins in colon, and higher-molecular-weight proteins (~200 kDa) in heart, lung, and testis. Therefore, of the rat tissues tested, the COOH-terminal epitope common to rb1NBC and rkNBC is predominantly expressed in kidney.

We also assessed the tissue distribution of rb2NBC using the same protocol as described above for rb1NBC. As observed after an ~2-s film exposure during chemiluminescence detection, αrb2NBC (1:2,000 dilution) strongly labeled an ~130-kDa protein, predominantly in brain but also in kidney (Fig. 4B). After an ~3-min film exposure (data not shown), the serum also labeled an ~130-kDa protein in liver. Therefore, of the rat tissues tested, the rb2NBC epitope is predominantly expressed in brain.

Localization of rb1NBC and rb2NBC in neurons and astrocytes. We also studied the cellular distribution of the two NBC clones in rat brain by performing immunoblots of protein isolated from neurons and astrocytes cultured from rat cortex. We separated microsomal proteins from cultured neurons and astrocytes by SDS-7.5% PAGE and then immunoblotted the protein with αrb1NBC or αrb2NBC . As a positive control, we also

¹ In other immunoblot experiments on rat brain protein, we often observed that αrb1NBC and αrb2NBC at higher concentrations (e.g., <1:1,000 dilution) labeled one or two other proteins in the 70- to 100-kDa range. The labeling of these other bands (i.e., not the ~70-kDa band in Fig. 3A) is specific because it can be competed away with the appropriate fusion proteins. These lower-molecular-weight proteins could be either breakdown products of rb1NBC and rb2NBC, or they could be smaller-sized NBCs. Multiple proteins are also labeled by an antibody to the COOH-terminal 108 AA of rkNBC (37).

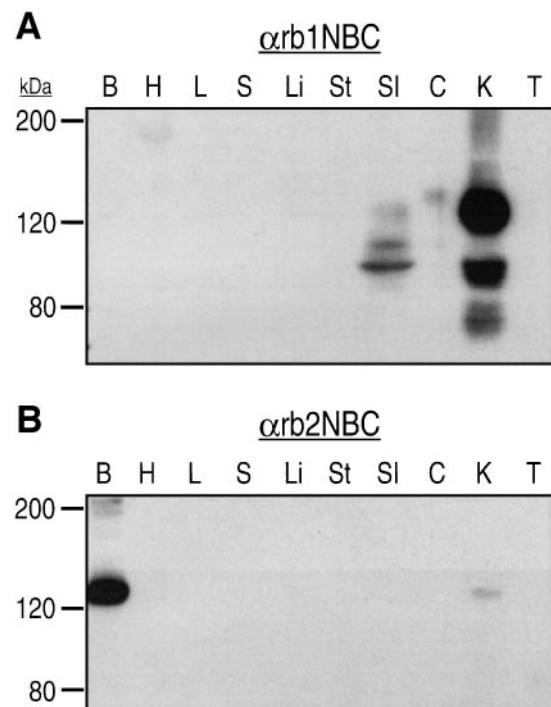


Fig. 4. αrb1NBC labels an ~130-kDa protein predominantly from kidney (A), whereas αrb2NBC labels an ~130-kDa protein predominantly from brain (B). αrb1NBC serum was diluted 1:1,000; αrb2NBC serum was diluted 1:2,000. Each lane contained ~80 μg total crude membrane protein isolated from tissues of an ~60-day-old male rat. Tissue abbreviations are as follows: B, brain; H, heart; L, lung; S, spleen; Li, liver; St, stomach; SI, small intestine; C, colon; K, kidney; T, testis.

immunoblotted protein from whole brain of rat. As shown in Fig. 5A, αrb1NBC labeled an ~130-kDa protein from astrocytes more intensely than from neurons. In contrast, αrb2NBC labeled an ~130-kDa protein from neurons more intensely than from astrocytes (Fig. 5B). Thus cultured neurons and astrocytes from rat cortex differentially express NBCs, with the COOH-terminus of rb1NBC being more prevalent in astrocytes and the COOH-terminus of rb2NBC being more prevalent in neurons.

Functional Characterization of rb2NBC Expressed in *Xenopus Oocytes*

Choi et al. (17) have shown that hpNBC expressed in *Xenopus oocytes* has all the basic properties expected of an electrogenic $\text{Na}^+\text{-HCO}_3^-$ cotransporter. Because rb1NBC is 96% identical to hpNBC, and because rb1NBC and hpNBC have almost identical NH_2 - and COOH-termini, we focused our attention in these functional studies on rb2NBC, which has a unique COOH-terminus.

Immunolabeling of rb2NBC expressed in *Xenopus oocytes*. We used αrb2NBC to confirm that oocytes injected with rb2NBC cRNA did in fact express rb2NBC protein. We used SDS-5% PAGE to separate total protein from oocytes injected with either H_2O or rb2NBC cRNA, or total protein from whole brain. As shown in Fig. 6, we then immunoblotted the protein using

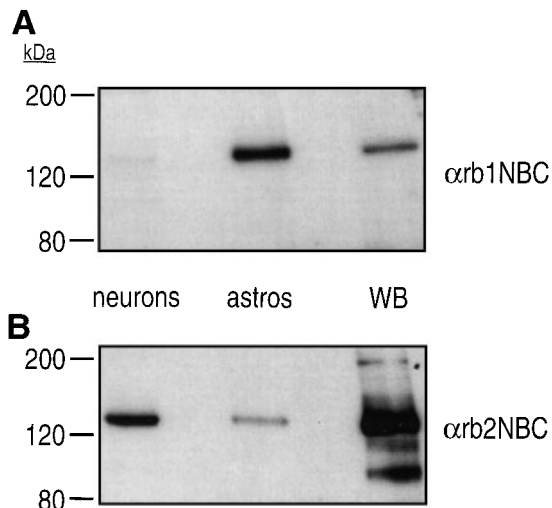


Fig. 5. Intensities of labeling by αrb1NBC and αrb2NBC are different in astrocytes and neurons cultured from rat cortex. *A*: αrb1NBC labeling of an ~ 130 -kDa protein is greater in the astrocytes (*lane 2*) than neurons (*lane 1*). αrb1NBC serum was diluted 1:1,000. *B*: αrb2NBC labeling of an ~ 130 -kDa protein is greater in the neurons (*lane 1*) than astrocytes (*lane 2*). αrb2NBC serum was diluted 1:5,000. Each lane in *A* and *B* contained ~ 7 μg total crude membrane protein. In *A* and *B*, the positive control was WB crude membrane protein (*lane 3*).

αrb2NBC . Our first approach for evaluating the specificity of labeling was to compare immunoblots for oocytes injected with H_2O with those for oocytes injected with rb2NBC cRNA. As expected, we found that αrb2NBC detected an ~ 130 -kDa protein in oocytes injected with rb2NBC (*lane 2*) but not in H_2O -injected oocytes (*lane 1*). Our second approach for evaluating the specificity of αrb2NBC labeling was to attempt to preabsorb the antibody with various fusion proteins. Preabsorption with the MBP- rb2NBC fusion protein eliminated the detection of the ~ 130 -kDa band from rb2NBC -expressing oocytes (*lane 3*). In contrast, preabsorption with MBP- rb1NBC did not reduce the intensity of the ~ 130 -kDa band (*lane 4*). For a positive control, we probed whole rat brain with αrb2NBC that we had pretreated with MBP- rb1NBC (*lane 5*). Thus, based on immunoblotting, rb2NBC protein is expressed in oocytes injected with rb2NBC cRNA.

Effect of applying $\text{CO}_2/\text{HCO}_3^-$ and removing external Na^+ . Figure 7*A* is a record of an experiment performed on an oocyte injected with cRNA encoding rb2NBC . In the standard ND-96 solution, the oocyte had a pH_i of ~ 7.3 and a V_m of approximately -55 mV (before *point a/a'*). Exposing the oocyte to a solution buffered with 1.5% $\text{CO}_2/10$ mM HCO_3^- elicited an initial pH_i decrease (*ab*), due to CO_2 influx, followed by a rapid pH_i recovery (*bc*), consistent with rb2NBC -mediated HCO_3^- transport into the oocyte. Applying $\text{CO}_2/\text{HCO}_3^-$ also elicited an abrupt hyperpolarization of ~ 40 mV (*a'b'*), consistent with transport of net negative charge into the cell. In the continued presence of $\text{CO}_2/\text{HCO}_3^-$, replacing external Na^+ with Li^+ had two effects. First, the replacement blocked the pH_i recovery and caused pH_i to decrease (*cd*). Second, the replacement elicited an abrupt depolarization (at *point c'*). Both findings are

consistent with reversal of an electrogenic NBC (4, 8, 17, 33, 34). We observed similar effects when we used either NMDG^+ or choline instead of Li^+ as the Na^+ substitute. In voltage-clamp experiments, Sciortino and Romero (40) have shown that Li^+ is only poorly transported by rkNBC expressed in *Xenopus* oocytes. Returning external Na^+ caused the pH_i to increase once again (*de*) and caused the oocyte to hyperpolarize (at *point d'*).

For comparison, Fig. 7*B* is a record of an experiment performed on a control oocyte injected with H_2O (rather than rb2NBC cRNA) but subjected to the same experimental protocol as the oocyte in Fig. 7*A*. Exposing a control oocyte to $\text{CO}_2/\text{HCO}_3^-$ elicited a rapid pH_i decrease due to CO_2 influx (*ab*), but there was no substantial pH_i recovery (*bc*). Also, applying $\text{CO}_2/\text{HCO}_3^-$ caused only a small depolarization (Fig. 7*B*, *a'b'*) in contrast to the large hyperpolarization observed in rb2NBC -expressing oocytes (Fig. 7*A*, *a'b'*). Replacing external Na^+ with NMDG^+ in the presence of $\text{CO}_2/\text{HCO}_3^-$ had little effect on pH_i (*cd*) and elicited only a small hyperpolarization (at *point c'*), consistent with the presence of a small Na^+ conductance.

In Fig. 7*C*, we summarize the effects on pH_i and V_m of applying $\text{CO}_2/\text{HCO}_3^-$ in experiments on rb2NBC -expressing and H_2O -injected oocytes such as those in Fig. 7, *A* and *B*. When oocytes are exposed to $\text{CO}_2/\text{HCO}_3^-$, the mean pH_i recovery rate from the initial CO_2 -induced acidification was 33-fold greater in rb2NBC -expressing oocytes than in H_2O -injected controls. Also, $\text{CO}_2/\text{HCO}_3^-$ elicited a mean hyperpolarization 30-fold greater in rb2NBC -injected oocytes than in H_2O -injected controls.

In Fig. 7*D*, we summarize the effects on pH_i and V_m of removing external Na^+ , as in Fig. 7, *A* and *B*. In Fig.

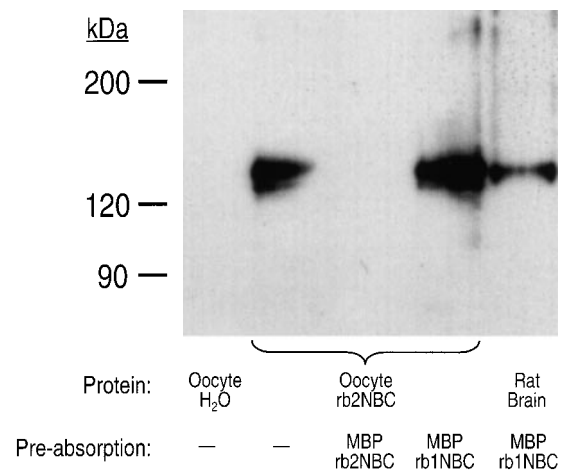


Fig. 6. *Xenopus* oocytes injected with rb2NBC cRNA express protein recognized by αrb2NBC . αrb2NBC does not label protein isolated from oocytes injected with H_2O (*lane 1*). In contrast, αrb2NBC labeled an ~ 130 -kDa protein from oocytes injected with rb2NBC cRNA (*lane 2*). The labeling was unaffected by preexposing αrb2NBC to MBP- rb1NBC (*lane 4*) but was prevented by preexposing αrb2NBC to MBP- rb2NBC (*lane 3*). As a positive control, αrb2NBC labeled an ~ 130 -kDa protein from rat brain protein, even after exposure to MBP- rb1NBC (*lane 5*). Lanes 1–4 contained equivalent amounts of protein from one oocyte. Lane 5 contained 2 μg rat brain crude membrane protein. Sera were diluted 1:2,000, and fusion proteins in the preabsorption lanes were used at 10 $\mu\text{g}/\text{ml}$.

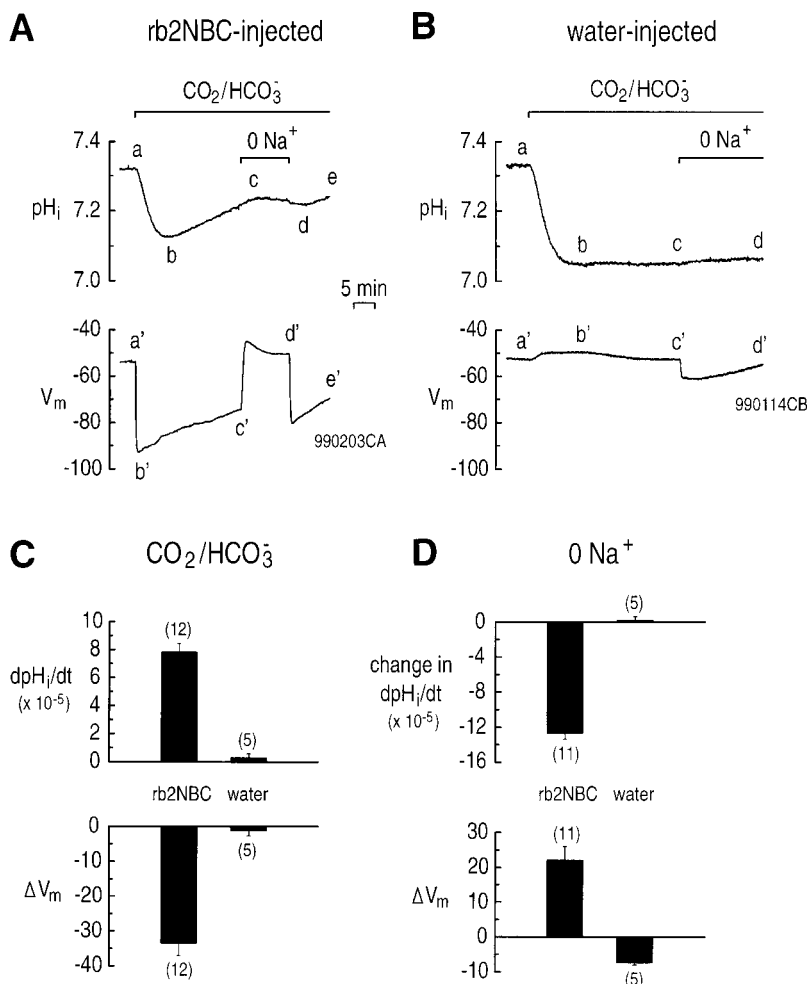


Fig. 7. rb2NBC expressed in *Xenopus* oocytes is electrogenic and Na^+ dependent. **A**: oocyte injected with rb2NBC cRNA. Applying 1.5% $\text{CO}_2/10 \text{ mM HCO}_3^-$ elicited a pH_i decrease (*ab*), followed by a gradual pH_i recovery (*bc*). Applying $\text{CO}_2/\text{HCO}_3^-$ also caused a large hyperpolarization (*a'b'*) that decayed slowly with time (*b'c'*). Removing external Na^+ in the continued presence of $\text{CO}_2/\text{HCO}_3^-$ inhibited the pH_i recovery (*cd*) and elicited an abrupt depolarization (at point *c'*). Returning the external Na^+ stimulated the pH_i recovery again (*de*) and caused the cell to hyperpolarize (at point *d'*). **B**: oocyte injected with water. The experimental protocol is similar to that shown in **A**. Applying 1.5% $\text{CO}_2/10 \text{ mM HCO}_3^-$ caused a pH_i decrease (*ab*), but no subsequent pH_i recovery (*bc*). Also, the $\text{CO}_2/\text{HCO}_3^-$ caused a small depolarization of the oocyte (*a'b'*). Removing external Na^+ had little effect on pH_i (*cd*) and elicited a small hyperpolarization (at point *c'*). **C**: summary data from experiments similar to those shown in **A** and **B** on the rate of pH_i recovery (dpH_i/dt) and change (Δ) in membrane potential (V_m) caused by applying $\text{CO}_2/\text{HCO}_3^-$ to oocytes injected with rb2NBC cRNA or water. **D**: summary data from experiments similar to those in **A** and **B** on the change in both dpH_i/dt and ΔV_m elicited by removing external Na^+ from oocytes injected with rb2NBC cRNA or water. A negative change in dpH_i/dt indicates an inhibition of the pH_i recovery. V_m is in units of mV, and dpH_i/dt is measured as pH units/s.

7D, top, the bars indicate the change in the rate of pH_i recovery (e.g., segments *cd-bc* in Fig. 7, **A** and **B**). In rb2NBC-expressing oocytes, Na^+ removal substantially reduced the pH_i recovery and, in fact, reversed it. On the other hand, in control oocytes, Na^+ removal had virtually no effect on the pH_i trajectory, which was flat to begin with. Also, removing Na^+ elicited a depolarization that averaged 22 mV in rb2NBC-injected oocytes, but a hyperpolarization that averaged 7 mV in control oocytes. The data in Fig. 7 are thus consistent with the hypothesis that rb2NBC is electrogenic and transports both Na^+ and HCO_3^- .

Effect of removing external Cl^- . Because some HCO_3^- -dependent acid-base transporters move Cl^- (e.g., Na^+ -dependent and -independent $\text{Cl}^-/\text{HCO}_3^-$ exchange), we performed the experiment shown in Fig. 8A to evaluate the Cl^- dependence of rb2NBC. The first part of the protocol was the same as that shown in Fig. 7A. After we had exposed the rb2NBC-injected oocyte to $\text{CO}_2/\text{HCO}_3^-$, removing external Na^+ elicited the expected pH_i decrease (*cd*) and depolarization (at point *c'*). If the pH_i decrease elicited by removing external Na^+ (and thereby reversing rb2NBC) were due to a Cl^- -dependent process such as a Na^+ -driven $\text{Cl}^-/\text{HCO}_3^-$ exchanger, then removing external Cl^- should block this pH_i decrease. However, removing and returning

external Cl^- had little effect on the pH_i decrease observed in the absence of external Na^+ (*cdef*). Returning Na^+ again elicited a pH_i recovery (*fg*) and also hyperpolarized the oocyte (at point *f'*). Switching back to the nominally $\text{CO}_2/\text{HCO}_3^-$ -free ND-96 solution reversed the pH_i (*gh*) and V_m (*g'h'*) effects produced by applying $\text{CO}_2/\text{HCO}_3^-$.

In Fig. 8B, we summarize segment *cf* pH_i decreases from four paired experiments similar to that in Fig. 8A. Rather than decreasing the rate of acidification, removing external Cl^- increased the rate by 50% ($P = 0.05$). We observed a similar increase in H_2O -injected controls (data not shown). Therefore, rb2NBC is neither a Na^+ -driven $\text{Cl}^-/\text{HCO}_3^-$ exchanger nor any other Cl^- -dependent transporter.

Effect of applying DIDS. Because most HCO_3^- -dependent transporters are sensitive to stilbene derivatives such as DIDS, we examined the effect of DIDS on rb2NBC. The experiment shown in Fig. 9A is similar to that shown in Fig. 7A and Fig. 8A in that we exposed an rb2NBC-expressing oocyte to $\text{CO}_2/\text{HCO}_3^-$ and then removed and returned external Na^+ . However, in Fig. 9A, we assessed the effect of 450 μM DIDS on the Na^+ -dependent changes of pH_i and V_m . As noted previously, returning the Na^+ elicited a pH_i recovery (*de*) and a hyperpolarization (at point *d'*). Exposing the oocyte to

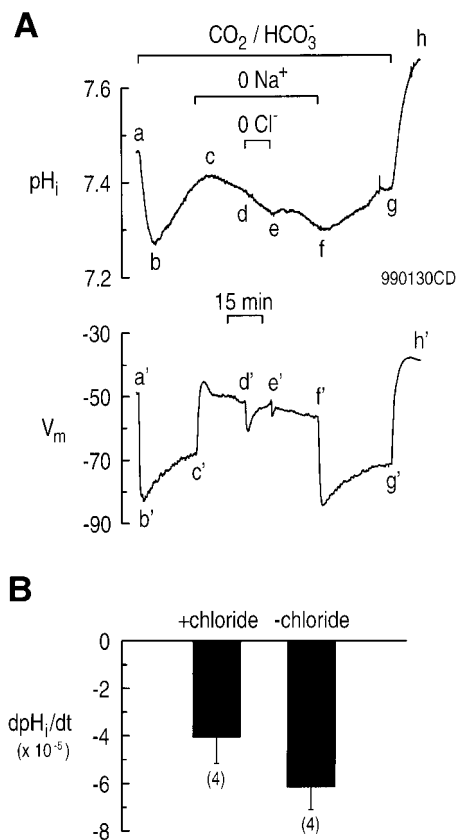


Fig. 8. rb2NBC expressed in *Xenopus* oocytes is Cl^- independent. *A*: oocyte injected with rb2NBC cRNA. Applying 1.5% $\text{CO}_2/10$ mM HCO_3^- elicited a pH_i decrease (*ab*), followed by a robust pH_i recovery (*bc*). Applying $\text{CO}_2/\text{HCO}_3^-$ also caused a large hyperpolarization (*a'b'*) that decayed slowly with time (*b'c'*). Removing external Na^+ in the continued presence of $\text{CO}_2/\text{HCO}_3^-$ inhibited the pH_i recovery and caused pH_i to decrease (*cd*). Removing Na^+ also elicited an abrupt depolarization (at point *c'*). Removing and returning external Cl^- in the absence of external Na^+ had little effect on the rate of pH_i decrease (*def*). Returning the external Na^+ stimulated the pH_i recovery again (*fg*) and caused the cell to hyperpolarize (at point *f'*). Subsequently, removing $\text{CO}_2/\text{HCO}_3^-$ elicited a pH_i increase (*gh*) and an abrupt depolarization (*g'h'*). *B*: summary data from 4 paired experiments similar to that shown in *A* on the rate of pH_i decrease (dpH_i/dt) elicited by first removing external Na^+ in the presence of Cl^- (+ Cl^-), and then removing external Cl^- in the continued absence of Na^+ (- Cl^-). V_m is in units of mV, and dpH_i/dt is measured as pH units/s.

450 μM DIDS not only blocked the pH_i recovery, but also unmasked a sizeable acidification (*ef*). The DIDS also elicited a depolarization (at point *e'*). Subsequently, removing external Na^+ in the presence of DIDS did not affect pH_i (*fg*) and generated only a small hyperpolarization (point *f'*) followed by a slow nonspecific depolarization to point *g'*.

In six paired experiments similar to that shown in Fig. 9A, the segment *de* pH_i recovery rate averaged $5.7 \pm 0.7 \times 10^{-5}$ pH units/s, and 450 μM DIDS reduced this figure during segment *ef* to a mean value of $1.9 \pm 1.2 \times 10^{-5}$ pH units/s; the difference between these values is statistically significant ($P = 0.007$). DIDS also depolarized the oocytes from an average of -73 ± 6 to -55 ± 5 mV ($P = 0.002$). In four paired experiments, we removed external Na^+ in both the absence and presence of DIDS. As summarized in Fig. 9B, top, Na^+

removal substantially slowed the pH_i recovery in the absence of DIDS ("control") but had virtually no effect in the presence of the inhibitor ("+DIDS"). Also, as summarized in Fig. 9B, bottom, removing external Na^+ caused a depolarization that averaged 23 mV in the absence of DIDS but a hyperpolarization that averaged 7 mV in the presence of DIDS. Thus DIDS blocks the function of rb2NBC.

DISCUSSION

97-bp Deletion of rb2NBC

In screening rat brain cDNA libraries and using 5'-RACE, we cloned two NBC-related cDNAs from rat brain. One clone, rb1NBC, is very similar to the NBC cloned from human pancreas and heart. The other clone, rb2NBC, is identical to rb1NBC except for a 97-bp deletion near the 3' end of the ORF, resulting in a protein with 61 novel COOH-terminal AA.

As to the origins of rb2NBC vs. rb1NBC, the most likely explanation is that rb2NBC is an alternative splice variant of rb1NBC in which an exon lacking the 97-bp region replaces an exon containing this region. Alternatively, the 97-bp segment is an intron that the splicing machinery fails to excise in the production of rb1NBC. However, the 5' and 3' termini of this 97-bp segment do not contain the well-conserved 5'-GT and 3'-AG consensus splice sequences found in the majority of premessenger RNA introns. The segment also lacks the 5'-AT and 3'-AC consensus splice sequences found in a small percentage of premessenger RNA introns (see Ref. 46). If this region is indeed an intron, then the 5' and 3' sequences may represent a new class of consensus splice sequences. Finally, rb1NBC and rb2NBC may represent different genes. Presumably, electrogenic NBCs have been localized to human chromosomes 4 (1, 32) and 17 (32).

Regardless of its origin, the 97-bp deletion causes a shift in the translational reading frame because 97 is not divisible by three. Consequently, the stop codon in rb2NBC is further 3' than that in rb1NBC, and the COOH-terminus of rb2NBC is unique. Although rare in eukaryotes, there are examples of such alternative splicing leading to a shift in the ORF. For example, an alternative splice variant of gastrin-releasing peptide contains an additional 19 nucleotides near the 3'-ORF, resulting in a translational frame shift and a unique COOH-terminus (44).

Novel COOH-Terminus of rb2NBC

According to our data, rb2NBC expressed in oocytes has the same general functional properties as akNBC (34), rkNBC (33), and hpNBC (17). Although we did not express and study the function of rb1NBC in oocytes, this clone is likely to be very similar in function to hpNBC, inasmuch as the two clones are 96% identical, and the 4% divergence is more-or-less evenly scattered throughout the clones. rkNBC, hpNBC, and rb2NBC are all electrogenic, Na^+ dependent, Cl^- independent, DIDS sensitive, and stimulated by applying $\text{CO}_2/\text{HCO}_3^-$ to the oocyte. The presence of the unique COOH-

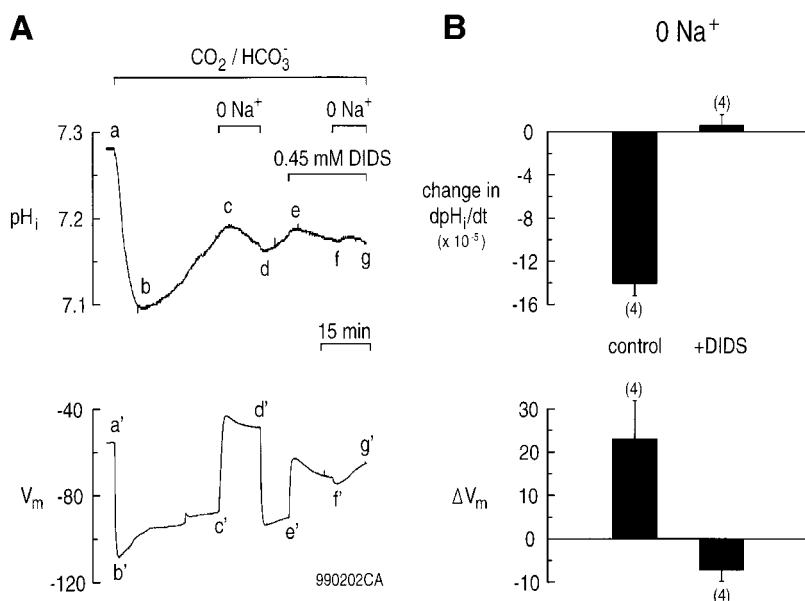


Fig. 9. rb2NBC expressed in *Xenopus* oocytes is DIDS sensitive. *A*: oocyte injected with rb2NBC cRNA. Applying 1.5% $\text{CO}_2/10 \text{ mM HCO}_3^-$ elicited a decrease and subsequent increase of pH_i (*abc*). Applying $\text{CO}_2/\text{HCO}_3^-$ also caused the expected hyperpolarization (*a'b'c'*). Removing external Na^+ in the continued presence of $\text{CO}_2/\text{HCO}_3^-$ inhibited the pH_i recovery and caused pH_i to decrease (*cd*). The onset of the pH_i decrease coincided with an abrupt depolarization (at point *c*). Returning external Na^+ reversed the pH_i decrease (*de*), and the cell hyperpolarized (at point *d*). Applying 450 μM DIDS inhibited the segment *de* pH_i recovery and caused pH_i to decrease (*ef*). DIDS also elicited a depolarization (at point *e*). Removing external Na^+ in the presence of DIDS had little effect on the pH_i decrease (*fg*) and elicited only a small hyperpolarization (point *f*) followed by a gradual depolarization to point *g*. *B*: summary data from 4 paired experiments similar to that shown in *A* on both the change in dpH_i/dt and ΔV_m elicited by removing external Na^+ in the absence (control) and presence (+DIDS) of DIDS. Negative change in dpH_i/dt indicates an inhibition of pH_i recovery. V_m is in units of mV, and dpH_i/dt is measured as pH units/s.

terminal 61 AA in rb2NBC compared with the comparable 46 AA in hpNBC does not obviously affect the function of the protein. However, our assays were not designed to detect more subtle differences between the clones. Thus it is possible that the COOH-terminus of NBC may affect such properties as affinities for transported ions or inhibitors, the V_{max} , or the voltage dependence.

Although rb2NBC expressed in oocytes is electrogenic, we do not know if the transporter has a $\text{Na}^+:\text{HCO}_3^-$ stoichiometry of 1:2 or 1:3. Based on the electrochemical gradients, an NBC with either stoichiometry would transport Na^+ and HCO_3^- into the oocyte. Determination of the $\text{Na}^+:\text{HCO}_3^-$ stoichiometry of rb2NBC (or rb1NBC) expressed in oocytes will require a more detailed study in which one compares at least two of the three following parameters in voltage-clamped oocytes: NBC-mediated Na^+ fluxes, HCO_3^- fluxes, and membrane currents.

The unique COOH-terminal 61 AA of rb2NBC are not homologous to any other sequence in GenBank. However, one interesting feature of this COOH-terminus is that the last three AA (TTL) resemble the COOH-terminal consensus sequence (S/TXV) that is recognized by PDZ domains of proteins that are involved in protein-protein interactions (see Ref. 23). PDZ is an acronym that stands for the first three proteins identified that contain conserved, 80–90 AA repeats that are involved in protein binding. These three proteins are a brain-specific synaptic protein (PSD-95), the *Drosophila* septate junction protein disks-large (Dlg), and the epithelial tight-junction protein zonula occludens-1 (ZO1). PDZ domains are found in proteins involved in signal transduction, and they may play a role in clustering other proteins in the plasma membrane (see Ref. 23). Although the COOH-terminal AA in rb2NBC is L rather than the V in the consensus sequence, there are examples in which the PDZ-binding domain contains an L instead of V. For example, LIN-7 of *Ca-*

norhabditis elegans, which is a component of the *ras*-signaling pathway, appears to interact with the COOH-terminal ETCL of the receptor tyrosine kinase LET-23 (41). Also, using a yeast two-hybrid screen, Strehler et al. (45) identified PDZ proteins that interact with the COOH-terminal ETSL of the 2b isoform of the plasma membrane $\text{Ca}^{2+}\text{-H}^+$ pump. Therefore, it is intriguing to speculate that the ETTL sequence in rb2NBC may be a PDZ-binding domain and may be important for either membrane targeting or functional regulation of rb2NBC.

Based on our functional studies, rb2NBC is expressed at the plasma membrane of oocytes. However, it is possible that NBCs such as rb1NBC and rb2NBC may also be expressed in intracellular compartments *in vivo*. Indeed, based on preliminary electron microscopy studies on rat brain slices, αrb1NBC appears to label intracellular proteins in neurons from rat cerebellum (A. Maunsbach, personal communication). We also cannot exclude the possibility that the subcellular localization of NBCs may vary among different brain regions.

Distribution of rb2NBC

As mentioned in the INTRODUCTION, considerable functional data demonstrate the existence of $\text{Na}^+\text{-HCO}_3^-$ cotransporters in both invertebrate and mammalian glia, particularly astrocytes. Indeed, as shown in Fig. 5, cultured cortical astrocytes strongly express the COOH-terminus of rb1NBC, but only weakly express rb2NBC. $\text{Na}^+\text{-HCO}_3^-$ cotransport has not been detected by function in neurons. Rather, in at least three neural preparations [the squid axon (9), the snail neuron (47), and the rat hippocampal neuron (38)] the Na^+ -driven $\text{Cl}^-/\text{HCO}_3^-$ exchanger appears to be the predominant Na^+ -dependent HCO_3^- transporter. According to the immunoblot data presented in this study, however, at least the COOH-terminus of the electrogenic rb2NBC is present in rat cortical neurons, which express, at most, very low levels of rb1NBC. In fact, rb2NBC appears to

be predominantly expressed in cultured cortical neurons compared with cortical astrocytes. We cannot rule out the possibility that αrb2NBC may also detect another HCO_3^- -dependent transporter (e.g., Na^+ -driven $\text{Cl}^-/\text{HCO}_3^-$ exchanger) that has an epitope similar to that recognized by the antibody. However, this other transporter would have to have approximately the same molecular weight as rb2NBC . Why are rb1NBC and rb2NBC expressed differently in neurons vs. astrocytes? Although these clones may have only subtle differences in function, their different COOH-termini may underlie more substantial differences in regulation and/or targeting. Recently, Schmitt et al. (36) have used both in situ hybridization and immunolocalization techniques to demonstrate the presence of NBC not only in astrocytes, but also in neurons from cortex, hippocampus, and periform cortex of rat. The probes used in these in situ hybridization and immunolocalization studies would be expected to recognize rb1NBC and rb2NBC .

The question arises as to the function of an electrogenic NBC in neurons. An electrogenic NBC with a $\text{Na}^+:\text{HCO}_3^-$ stoichiometry of 1:2 would probably function as an acid extruder and raise pH_i at all physiological V_m (40) and would probably be accelerated at the positive V_m accompanying an action potential. Even an NBC with a 1:3 stoichiometry would transport Na^+ and HCO_3^- into the cell during action potentials. However, most experimenters have observed that neuronal firing causes a decrease in pH_i rather than an increase (see Ref. 3). The major causes of these pH_i decreases are the influx of H^+ mediated by the $\text{Ca}^{2+}\text{-H}^+$ pump and the efflux of HCO_3^- mediated by the GABA_A channel. If electrogenic $\text{Na}^+\text{-HCO}_3^-$ cotransport is indeed stimulated during neuronal firing, then this cotransporter may minimize the extent of the activity-induced decrease in pH_i and concomitant increase in pH_{ECF} . Thus electrogenic NBCs in both neurons and glial cells may influence the extent to which pH_i and pH_{ECF} change in response to neuronal firing. In addition, these NBCs may have different functional properties and sensitivities to various signaling pathways and may thus respond differently to a range of electrical and chemical stimuli.

NOTE ADDED IN PROOF

Giffard et al. recently reported the cloning of an NBC (GenBank accession number AF210250) from a rat brain hippocampal cDNA library (Giffard RG, Papadopoulos MC, van Hooft JA, Xu L, Giuffrida R, and Monyer H. The electrogenic sodium bicarbonate cotransporter: developmental expression in rat brain and possible role in acid vulnerability. *J Neurosci* 20: 1001–1008, 2000). The translated protein is identical to rb1NBC , except for four amino acids.

We thank Dr. Terry P. Snutch (Biotechnology Laboratory, Univ. of British Columbia) for kindly allowing us to use the $\lambda\text{RB-L}$ cDNA library, William J. Joiner (Kaczmarek Laboratory, Dept. of Pharmacology, Yale University) for providing us with the $\lambda\text{RB-L}$ cDNA library and for assisting in the library screening, Drs. Ying Xia and Gabriel G. Haddad (Dept. of Pediatrics, Yale University) for generously providing us with cultured cortical neurons, Dr. Christopher B. Burge

(Center for Cancer Research, Massachusetts Institute of Technology) for helping us analyze the clones, and Duncan Wong for providing computer support.

M. O. Bevensee was supported by National Institutes of Health (NIH) Training Grant TG HL-07778. B. M. Schmitt was supported by a Forschungsstipendium from the Deutsche Forschungsgemeinschaft. I. Choi was supported by a postdoctoral fellowship from the American Heart Association. M. F. Romero was supported by NIH Service Award DK-09342 and by a grant from the American Heart Association. This work was supported by NIH Grants P01 HD-32573 and DK-30344.

GenBank accession numbers are AF254802 for rb1NBC and AF124441 for rb2NBC .

Present addresses: B. M. Schmitt, Dept. of Anatomy, University of Würzburg, 97070 Würzburg, Germany; M. F. Romero, Dept. of Physiology and Biophysics, Case Western Reserve University School of Medicine, Cleveland, OH 44106-4970.

Address for reprint requests and other correspondence: M. O. Bevensee, Dept. of Cellular and Molecular Physiology (12-17-99), Yale Univ. School of Medicine, 333 Cedar St., Rm. B-127 SHM, New Haven, CT 06520.

Received 3 September 1999; accepted in final form 30 December 1999.

REFERENCES

1. **Abuladze N, Lee I, Newman D, Hwang J, Boorer K, Pushkin A, and Kurtz I.** Molecular cloning, chromosomal localization, tissue distribution, and functional expression of the human pancreatic sodium bicarbonate cotransporter. *J Biol Chem* 273: 17689–17695, 1998.
2. **Amlal H, Burnham CE, and Soleimani M.** Characterization of $\text{Na}^+\text{-HCO}_3^-$ cotransporter isoform NBC-3. *Am J Physiol Renal Physiol* 276: F903–F913, 1999.
3. **Ballanyi K and Kaila K.** Activity-evoked changes in intracellular pH. In: *pH and Brain Function*, edited by Kaila K and Ransom BR. New York: Wiley-Liss, 1998, p. 291–308.
4. **Bevensee MO, Apkon M, and Boron WF.** Intracellular pH regulation in cultured astrocytes from rat hippocampus. II. Electrogenic Na/HCO_3 cotransport. *J Gen Physiol* 110: 467–483, 1997.
5. **Bevensee MO and Boron WF.** pH regulation in mammalian neurons. In: *pH and Brain Function*, edited by Kaila K and Ransom BR. New York: Wiley-Liss, 1998, p. 211–231.
6. **Bevensee MO, Schmitt BM, Romero MF, and Boron WF.** Cloning of a putative Na/HCO_3 cotransporter (NBC) from rat brain (Abstract). *FASEB J* 12: A1031, 1998.
7. **Bevensee MO, Weed RA, and Boron WF.** Intracellular pH regulation in cultured astrocytes from rat hippocampus. I. Role of HCO_3^- . *J Gen Physiol* 110: 453–465, 1995.
8. **Boron WF and Boulpaep EL.** Intracellular pH regulation in the renal proximal tubule of the salamander: basolateral HCO_3^- transport. *J Gen Physiol* 81: 53–94, 1983.
9. **Boron WF and Russell JM.** Stoichiometry and ion dependencies of the intracellular-pH-regulating mechanism in squid giant axons. *J Gen Physiol* 81: 373–399, 1983.
10. **Boyersky G, Ransom B, Schlue W-R, Davis MBE, and Boron WF.** Intracellular pH regulation in single cultured astrocytes from rat forebrain. *Glia* 8: 241–248, 1993.
11. **Burnham CE, Amlal H, Wang Z, Shull GE, and Soleimani M.** Cloning and functional expression of a human kidney $\text{Na}^+:\text{HCO}_3^-$ cotransporter. *J Biol Chem* 272: 19111–19114, 1997.
12. **Burnham CE, Flagella M, Wang Z, Amlal H, Shull GE, and Soleimani M.** Cloning, renal distribution, and regulation of the rat $\text{Na}^+\text{-HCO}_3^-$ cotransporter. *Am J Physiol Renal Physiol* 274: F1119–F1126, 1998.
13. **Chen JC and Chesler M.** A bicarbonate-dependent increase in extracellular pH mediated by GABA_A receptors in turtle cerebellum. *Neurosci Lett* 116: 130–135, 1990.
14. **Chen JCT and Chesler M.** Extracellular alkaline shifts in rat hippocampal slice are mediated by NMDA and non-NMDA receptors. *J Neurophysiol* 68: 342–344, 1992.
15. **Chesler M.** The regulation and modulation of pH in the nervous system. *Prog Neurobiol* 34: 401–427, 1990.

16. **Choi I, Aalkjaer C, Boulpaep EL, and Boron WF.** An electro-neutral Na/bicarbonate cotransporter (NBCn1) and associated sodium channel. *Nature*. In press.
17. **Choi I, Romero MF, Khandoudi N, Bril A, and Boron WF.** Cloning and characterization of a human electrogenic Na⁺-HCO₃⁻ cotransporter isoform (hhNBC). *Am J Physiol Cell Physiol* 276: C576–C584, 1999.
18. **Deitmer JW.** pH regulation in invertebrate glia. In: *pH and Brain Function*, edited by Kaila K and Ransom BR. New York: Wiley-Liss, 1998, p. 233–252.
19. **Deitmer JW and Rose CR.** pH regulation and proton signalling by glial cells. *Prog Neurobiol* 48: 73–103, 1996.
20. **Deitmer JW and Schlue W-R.** The regulation of intracellular pH by identified glial cells and neurones in the central nervous system of the leech. *J Physiol (Lond)* 388: 261–283, 1987.
21. **Deitmer JW and Schlue W-R.** An inwardly directed electrogenic sodium-bicarbonate cotransport in leech glial cells. *J Physiol (Lond)* 411: 179–194, 1989.
22. **Douglas RM, Xia Y, Schmitt BM, Bevensee MO, Biemesderfer D, Boron WF, and Haddad GG.** Developmental and stress-induced profile of two CNS pH regulatory proteins: the Na/H exchanger and the Na/HCO₃⁻ cotransporter (Abstract). *Abstr Soc Neurosci* 24: 1605, 1998.
23. **Fanning AS and Anderson JM.** PDZ domains and the formation of protein networks at the plasma membrane. *Curr Top Microbiol Immunol* 228: 209–233, 1998.
24. **Giffard RG, Emond MR, Giuffrida R, and Monyer H.** Identification and cloning of a new protein from rat brain related to the sodium bicarbonate cotransporter (Abstract). *Abstr Soc Neurosci* 24: 1504, 1998.
25. **Kaila K, Paalasmaa P, Taira T, and Voipio J.** pH transients due to monosynaptic activation of GABA-A receptors in rat hippocampal slices. *Neuroreport* 3: 105–108, 1992.
26. **Kaila K and Voipio J.** Postsynaptic fall in intracellular pH induced by GABA-activated bicarbonate conductance. *Nature* 330: 163–165, 1987.
27. **Paalasmaa P and Kaila K.** Role of voltage-gated calcium channels in the generation of activity-induced extracellular pH transients in the rat hippocampal slice. *J Neurophysiol* 75: 2354–2360, 1996.
28. **Paalasmaa P, Taira T, Voipio J, and Kaila K.** Extracellular alkaline transients mediated by glutamate receptors in the rat hippocampal slice are not due to a proton conductance. *J Neurophysiol* 72: 2031–2033, 1994.
29. **Pushkin A, Abuladze N, Lee I, Newman D, Hwang J, and Kurtz I.** Cloning, tissue distribution, genomic organization, and functional characterization of NBC3, a new member of the sodium bicarbonate cotransporter family. *J Biol Chem* 274: 16569–16575, 1999.
30. **Raley-Susman KM, Cragoe EJ Jr, Sapolsky RM, and Kopito RR.** Regulation of intracellular pH in cultured hippocampal neurons by an amiloride-insensitive Na⁺/H⁺ exchanger. *J Biol Chem* 266: 2739–2745, 1991.
31. **Ransom BR.** Glial modulation of neural excitability mediated by extracellular pH: a hypothesis. *Prog Brain Res* 94: 37–46, 1992.
32. **Romero MF, Davis BA, Sussman CR, Bray-Ward P, Ward D, and Boron WF.** Identification of multiple genes for human electrogenic Na/HCO₃⁻ cotransporters (NBC) on 4q (Abstract). *J Am Soc Nephrol* 9: 11A, 1998.
33. **Romero MF, Fong P, Berger UV, Hediger MA, and Boron WF.** Cloning and functional expression of rNBC, an electrogenic Na⁺-HCO₃⁻ cotransporter from rat kidney. *Am J Physiol Renal Physiol* 274: F425–F432, 1998.
34. **Romero MF, Hediger MA, Boulpaep EL, and Boron WF.** Expression cloning and characterization of a renal electrogenic Na⁺/HCO₃⁻ cotransporter. *Nature* 387: 409–413, 1997.
35. **Rose CR and Ransom BR.** pH regulation in mammalian glia. In: *pH and Brain Function*, edited by Kaila K and Ransom BR. New York: Wiley-Liss, 1998, p. 253–275.
36. **Schmitt BM, Bevensee MO, Douglas R, Berger UV, Hediger MA, Haddad G, and Boron WF.** Expression and localization of Na⁺/HCO₃⁻ cotransporter (NBC) mRNA and protein in rat brain (Abstract). *Abstr Soc Neurosci* 24: 1066, 1998.
37. **Schmitt BM, Biemesderfer D, Romero MF, Boulpaep EL, and Boron WF.** Immunolocalization of the electrogenic Na⁺/HCO₃⁻ cotransporter in mammalian and amphibian kidney. *Am J Physiol Renal Physiol* 276: F27–F36, 1999.
38. **Schwiening CJ and Boron WF.** Regulation of intracellular pH in pyramidal neurons from the rat hippocampus by Na⁺-dependent Cl⁻-HCO₃⁻ exchange. *J Physiol (Lond)* 475: 59–67, 1994.
39. **Schwiening CJ, Kennedy HJ, and Thomas RC.** Calcium-hydrogen exchange by the plasma membrane Ca-ATPase of voltage-clamped snail neurons. *Proc R Soc Lond B Biol Sci* 253: 285–289, 1993.
40. **Sciortino CM and Romero MF.** Cation and voltage dependence of the rat kidney, electrogenic Na⁺/HCO₃⁻ cotransporter, expressed in *Xenopus* oocytes. *Am J Physiol Renal Physiol* 277: F611–F623, 1999.
41. **Simske JS, Kaech SM, Harp SA, and Kim SK.** LET-23 receptor localization by the cell junction protein LIN-7 during *C. elegans* vulval induction. *Cell* 85: 195–204, 1996.
42. **Smith SE, Gottfried JA, Chen JCT, and Chesler M.** Calcium dependence of glutamate receptor-evoked alkaline shifts in hippocampus. *Neuroreport* 5: 2441–2445, 1994.
43. **Somjen GG and Tombaugh GC.** pH modulation of neuronal excitability and central nervous system functions. In: *pH and Brain Function*, edited by Kaila K and Ransom BR. New York: Wiley-Liss, 1998, p. 373–393.
44. **Spindel ER, Zilberberg MD, Habener JF, and Chin WW.** Two prohormones for gastrin-releasing peptide are encoded by two mRNAs differing by 19 nucleotides. *Proc Natl Acad Sci USA* 83: 19–23, 1986.
45. **Strehler EE, Scarisbrick IA, and DeMarco SJ.** The plasma membrane calcium ATPase isoform 2B binds to membrane cytoskeleton-associated PDZ domain proteins (Abstract). *Abstr Soc Neurosci* 24: 1801, 1998.
46. **Tarn W-Y and Steitz JA.** Pre-mRNA splicing: the discovery of a new spliceosome doubles the challenge. *Trends Biochem Sci* 22: 132–137, 1997.
47. **Thomas RC.** The role of bicarbonate, chloride and sodium ions in the regulation of intracellular pH in snail neurones. *J Physiol (Lond)* 273: 317–338, 1977.
48. **Trapp S, Lückermann M, Kaila K, and Ballanyi K.** Acidosis of hippocampal neurones mediated by a plasmalemmal Ca²⁺/H⁺ pump. *Neuroreport* 7: 2000–2004, 1996.
49. **Traynelis SF.** pH modulation of ligand-gated ion channels. In: *pH and Brain Function*, edited by Kaila K and Ransom BR. New York: Wiley-Liss, 1998, p. 417–446.
50. **Xia Y, O'Reilly JP, and Haddad GG.** Prolonged hypoxia increases Na⁺ channel density in cultured rat neocortical neurons (Abstract). *Abstr Soc Neurosci* 22: 2151, 1996.